Anodic Hydrogen Generation from Benzaldehyde on Au, Ag, and Cu: Rotating Ring-Disk Electrode Studies

Nathanael C Ramos[1,2], Hudson Neyer[1,2], J Will Medlin[1], Adam Holewinski[1,2,z]

[1]Department of Chemical and Biological Engineering, University of Colorado Boulder, JSCBB, 3415 Colorado Avenue, Boulder, Colorado 80303, United States
[2]Renewable and Sustainable Energy Institute, University of Colorado Boulder, SEEC, 4001 Discovery Dr, Boulder, Colorado 80309, United States
[z]adam.holewinski@colorado.edu

Abstract

Aldehydes are selectively oxidized to carboxylates on group 11 metals at low potentials (<0.4 V vs. RHE) in alkaline media. This process can occur by a pathway that generates H_2 gas from the aldehyde, known as electro-oxidative dehydrogenation (EOD) or anodic hydrogen production. The EOD process occurs with transfer of only one electron per aldehyde, whereas typical oxidation with discharge of hydrogen to form water is a two-electron process. Here, we study the catalytic activity and selectivity toward H_2 of Au, Ag, and Cu electrodes using benzaldehyde with rotating disk and ring-disk electrode (RDE/RRDE) techniques. The average number of electrons per benzaldehyde molecule obtained via H_2 detection by RRDE agrees with that obtained via Koutecký-Levich analysis conducted at various rotation rates. We find that Au and Ag have much higher H_2 and benzoate formation rates than Cu, but that Cu can perform the reaction at about 0.2 V lower overpotentials. On all three materials, benzaldehyde oxidation has high selectivity to anodic H_2 (one-electron pathway) below ~0.5 V vs. RHE, but, with increasing potential, the selectivity shifts to H-oxidation forming water (two-electron pathway).

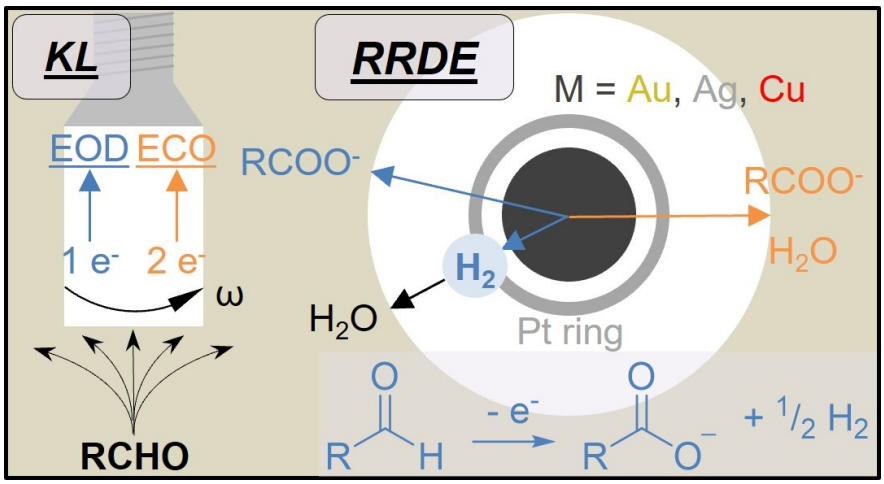

Introduction

Hydrogen is a key reactant in many chemical processes (e.g., ammonia synthesis, hydrogenation reactions, Fischer-Tropsch, etc.), and it can also be used as a green fuel.[1] Water electrolysis powered by renewable electricity can produce hydrogen via the hydrogen evolution reaction (HER) at the cathode. Although promising, electrolysis technology is not developed enough to compete with the cost of fossil fuel-derived hydrogen. Electrolysis is thermodynamically and kinetically limited by the oxygen evolution reaction (OER) at the anode, incurring high electricity costs that cannot be offset by oxygen, a low value product. Biomass-derived organic oxidation reactions are thus increasingly being investigated as alternatives to OER that could reduce the cost of green hydrogen and provide valuable anode products.[2]

Electrocatalytic oxidative dehydrogenation (EOD) of biomass-derived aldehydes (Equation 1) is a particularly intriguing alternative anode reaction:

$$\text{EOD: } RCHO + 2\ OH^- \rightarrow RCOO^- + H_2O + \tfrac{1}{2}\ H_2 + e^- \qquad (1)$$

Favored in alkaline media, the EOD pathway can selectively transform aldehydes into carboxylates while simultaneously producing H_2 gas at the *anode*, at potentials positive of the equilibrium potential for standard hydrogen oxidation.[3] This one-electron pathway stands in contrast to the more common two-electron pathway ("standard" electrochemical oxidation, ECO, equation 2):

$$\text{ECO: } RCHO + 3\ OH^- \rightarrow RCOO^- + 2\ H_2O + 2\ e^- \qquad (2)$$

Au, Ag, and Cu anodes are established to prefer the EOD pathway at low overpotentials[4] while other simple metal electrocatalysts generally oxidize hydrogen to H_2O and therefore primarily catalyze ECO.[5] At higher potentials, oxidation of (presumptively) adsorbed hydrogen (reverse Volmer reaction) becomes more kinetically favorable, and higher organic oxidation products (e.g., CO_2) may also be obtained, reducing the selectivity and electron efficiency of organic product formation.[6]

Anodic hydrogen was observed at least as early as the 1980s, primarily as a product of formaldehyde oxidation.[7–9] EOD has regained interest due to the possibility of utilizing biomass-derived (carbon neutral) reactants and producing dual-electrode hydrogen at scale with low costs for materials (copper electrodes) and electricity (low cell voltage). In 2020, Wang and coworkers demonstrated high selectivity (~100% FE to H_2) at industrially relevant current density (100 mA/cm^2) and low cell voltage (0.27 V) during oxidation of 5-hydroxymethylfurfural (HMF) to 5-hydroxymethyl-2-furancarboxylic acid, (HMFCA) on a roughened Cu foam anode.[10] Higher activity than monometallic Cu has been achieved primarily with Cu-based bimetallics such as CuAg[5] and CuPt.[11]

Despite existing research, the reaction mechanism of EOD still requires clarification. In alkaline media, aldehydes undergo base-mediated hydration, forming gem-diol and gem-diolate in solution.[12] This chemical equilibrium is proposed to enable dehydrogenation at low potentials due to weakening of the C-H bond and, therefore, surface-mediated OH-addition may not be required.[5,10] Additionally, it is inferred that to observe high selectivity to anodic hydrogen at 0.1-0.4 V_{RHE}, the kinetic barrier for the Volmer reaction ($H^* + OH^- \rightarrow * + H_2O + e^-$) under these conditions must be high compared to the Tafel reaction ($H^* + H^* \rightarrow H_2 + 2^*$), assuming that H* is an intermediate in this reaction. Lastly, despite numerous studies of EOD with formaldehyde reported on Au and Ag,[7] the intrinsic activity and selectivity of monometallic group 11 metals (including Cu) have not been compared under equal conditions with most prototypical aldehydes. Formaldehyde is unique in that it has two aldehyde-like hydrogens and can decompose thermally to CO and H_2, enabling anodic current efficiency toward H_2 to nominally exceed 100%.[4] A fair comparison of intrinsic activity and selectivity on Au, Ag, and Cu can be made using catalysts with well-defined surface area, negligible or well-characterized mass transport, and a model aldehyde with minimal propensity toward homogeneous side reactions. By understanding the reaction mechanism and activity and selectivity trends on model surfaces, one might more rationally design a reaction scheme with optimal catalyst, electrolyte, and mass transfer conditions to maximize H_2 production and minimize cost.

Here, we study benzaldehyde oxidation in alkaline media on Au, Ag, and Cu electrodes using rotating disk electrode (RDE) methods. The RDE allows deconvolution of mass transfer from kinetics and, for well-characterized or well-defined materials, permits direct comparisons and benchmarking of performance. Specifically, we quantify the product formation rates (hydrogen and carboxylate) and hydrogen selectivity by two complementary measurements. First, hydrogen generated via EOD is detected by the hydrogen oxidation reaction (HOR) using a concentric Pt ring electrode (rotating ring-disk electrode, RRDE). Second, currents are measured at multiple rotation rates and fit to the Koutecký-Levich equation to extract the average number of electrons per aldehyde converted (EOD: H_2, 1 e^-; ECO: H_2O, 2 e^-). In one case, H_2 oxidation on the RRDE must be isolated in the presence of interfering organic species; in the other case (Koutecký-Levich analysis) the reaction must reach a regime of mass transfer influence (high activity), which not all materials achieve. We find that each method provides similar quantitative results for cases where both can be performed, providing a valuable benchmark for studies in only one of the techniques can be applied. We use these two methods to show that anodic hydrogen selectivity decreases as a function of potential and that specific formation rates of hydrogen and carboxylate are much higher on Au and Ag compared to Cu.

Experimental

Chemicals

All chemicals were used as purchased without further purification. All electrolytes were prepared in ultrapure deionized water (>18.2 MΩ cm, Millipore). Solutions were prepared with sodium hydroxide (Sigma-Aldrich, >99.99% trace metals basis) and purged of oxygen with argon (UHP, AirGas) or hydrogen (UPC, AirGas). Benzaldehyde (Sigma-Aldrich, ReagentPlus® ≥99%) and/or sodium benzoate (Sigma-Aldrich, BioXtra >99.5%) were added to the electrolyte to reach concentrations noted with each experiment.

Electrochemical equipment and experimental apparatus

Electrochemical data acquisition was done on a Biologic SP-300 potentiostat. A Pine Research MSR Rotator was used for all experiments, with a Pine Research PTFE E5TQ ChangeDisk RDE tip or E6R1 ChangeDisk RRDE tip (Pt ring OD 7.5 mm, ID 6.5 mm) and Au, Ag, or Cu (5 mm OD) disk inserts. The reference electrode was a Hg/HgO couple in 4.24 M KOH (Koslow Scientific Company). The potential of the reference electrode was measured in electrolyte (without organic) versus a hydrogen reference electrode (Gaskatel Hydroflex). All potentials are quoted in V vs. reversible hydrogen electrode (RHE). Solution resistance was not compensated during or after the experiment but was typically measured to be 40 Ω and would not significantly influence results (< 10 mV shift at maximum currents). The counter electrode was a graphite rod (Thermo Scientific, 99.9995% metals basis). A glass RDE cell was used for all experiments (for ease of diagnosing and resolving issues with bubbles on the R/RDE interface), but Koutecký-Levich experiments were also conducted in a PTFE cell (all components glass free) to confirm that dissolution of silica from glass in alkaline electrolyte[13] did not significantly impact the electrochemistry. No significant differences were found in the number of electrons transferred (i.e., H_2 selectivity) or in the activity trends.

Prior to each experiment the cell was rinsed thoroughly with water, then soaked with boiling water three times. Disk electrodes were polished each time to similar low roughness to facilitate comparison across samples. Each electrode was polished to a mirror finish with 0.05 μm alumina (Allied High Tech) followed by rinsing and sonicating in water for 5 minutes. As necessary, 1 μm and 0.3 μm alumina were first used to polish out any visual surface defects.

Rotating Ring-Disk Electrode Procedure

The electrolyte was deaerated using Ar, and the Pt ring was first activated (with the Au/Ag/Cu disk under potential control at 0 V) for 30 cyclic voltammetry (CV) cycles from 0.05 to 1.4 V at 300 mV/s. Then, the Au/Ag/Cu disk was subjected to activation cycling with the Pt ring potential held at 1.4 V (to prevent disk metal deposition on the Pt ring). Each disk was cycled at 300 mV/s until a stable CV was obtained (Au: 0 to 1.55 V; Ag: -0.2 to 1.1 V; Cu: 0 to 0.65 V). The Pt ring was then shifted to 0.25 V for H_2 collection during the remainder of each experiment. In each trial, a background CV was acquired at 1600 RPM and 10 mV/s in the same potential region as the initial cycling. The disk was then held at 0 V during potential

controlled addition of benzaldehyde to the cell. Once the benzaldehyde was fully dissolved (5-10 min), CVs were repeatedly conducted at 1600 RPM and 10 mV/s. The stable CV (usually setting in by cycle 3-5) is presented.

Koutecký-Levich experiments were conducted within the same general experimental setup as the RRDE experiments after a stable 1600 RPM CV was acquired. The CVs were taken at 10 mV/s in the order of 1600, 900, 400, and 100 RPM between 0 to 1.55 V or -0.2 to 1.1 V for Au and Ag, respectively. The average number of electrons per aldehyde consumed (and thus selectivity to the anodic H_2 pathway) was obtained from the mass transfer limiting current term of the fitted Koutecký-Levich equation with measured currents at different rotation rates. Cu did not reach mass transfer limitations (evidenced by RPM-independence of the CVs) under these experimental conditions and therefore Koutecký-Levich analysis was not performed for this material.

Results and Discussion

Reaction on Au

Benzaldehyde was chosen as a model aldehyde molecule to probe trends in the activity and selectivity of EOD across materials. Benzaldehyde is established to generate anodic H_2 under appropriate conditions[10] and is less susceptible to polymerization side reactions than biomass-derived furans like furfural and HMF.[14,15] Moderate alkaline conditions were chosen (pH ~13, 0.1 M NaOH) along with low aldehyde concentrations (<10 mM) in order to minimize the effects of the Cannizzaro reaction between aldehydes and directly probe the EOD process.[5,10]

CV was used to characterize benzaldehyde oxidation under different mass transfer conditions using the RDE and RRDE techniques (Figure 1). Benzaldehyde oxidation begins at around 0.25 V and reaches a current plateau by 0.7 V at 1600 RPM. Upon reaching about 1.3 V, Au becomes inactive. On the reverse sweep, Au does not regain activity until 1.2 V. The inactivity and hysteresis at high potentials correspond to the potential region of gold oxide formation and reduction, suggesting that the gold surface oxide is inactive for benzaldehyde oxidation. The current plateau mainly aligns with the two-electron mass transfer limiting current of benzaldehyde based on the Levich equation (equation 3):

$$\mathrm{I_{MT,lim}} = 0.62\mathrm{nFA_{geom}D_{RCHO}^{2/3}\nu^{-1/6}\omega^{1/2}C_{RCHO}} \quad (3)$$

where n is the number of electrons transferred per reactant, F is Faraday's constant (96485 C/mol), A_{geom} is geometric area of the RDE (0.196 cm^2), D is the diffusion coefficient of benzaldehyde in water (0.816 x 10^{-5} cm^2/s at 22 °C),[16] ν is the kinematic viscosity of the solution (0.914 x 10^{-2} cm^2/s for 0.1 M NaOH at 25 °C),[17] ω is rotation rate, and C is concentration of benzaldehyde. The number of electrons transferred, n, describes the selectivity between the EOD (1 e^-) and ECO (2 e^-) pathways. As discussed below, the

selectivity at the plateau is not necessarily indicative of behavior at lower potential. An inflection point can be seen around 0.5 V, which we will shortly show relates to a shift in the dominant pathway.

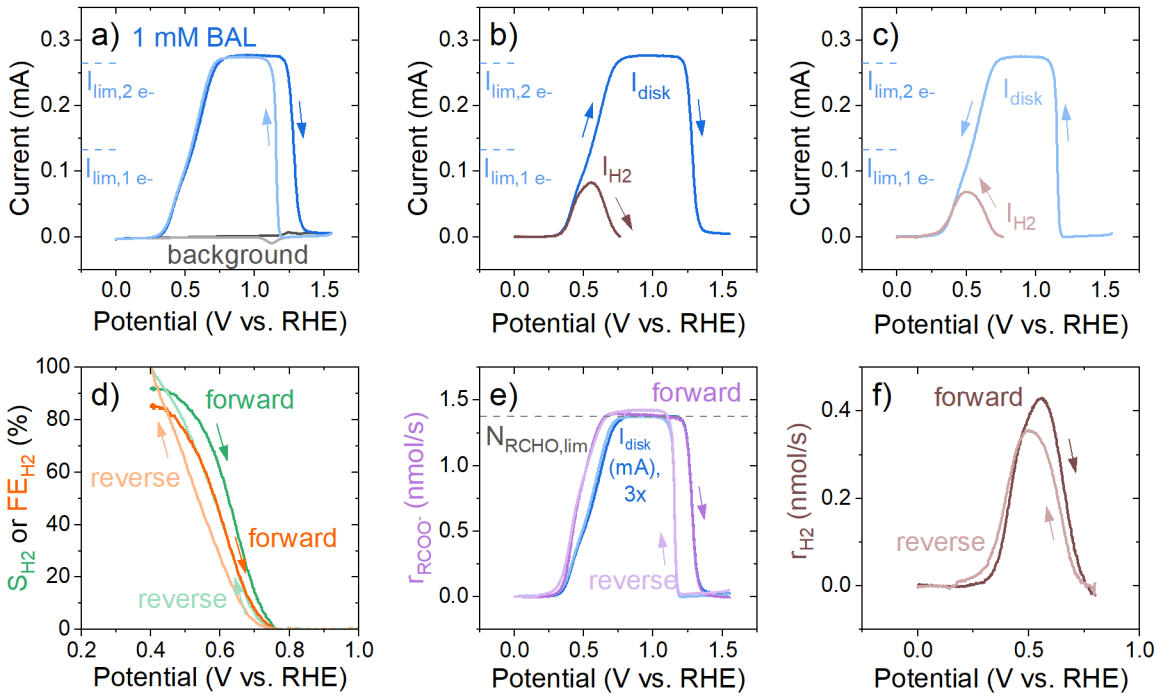

Figure 1. Au disk - Pt ring RRDE measurements in 0.1 M NaOH + 1 mM benzaldehyde. Darker curves are forward sweep; lighter curves are reverse sweep. (a) Au disk CV at 10 mV/s comparing background (black) and benzaldehyde (blue) in electrolyte at 1600 RPM. Dashed lines show the theoretical mass transfer limiting currents for the one-electron (H_2) and two-electron (H_2O) reaction pathways. (b) Forward sweep and (c) reverse sweep showing Au disk current (blue) and partial current density (brown) to H_2 pathway calculated from Pt ring current. (d) Selectivity (green) and Faradaic efficiency (orange) to the one-electron (H_2) reaction pathway. (e) Rate of carboxylate product formation (purple); black dashed line is the maximum mass transfer rate of aldehyde to the surface; disk current (blue) is replotted for reference and rescaled for ease of comparison. (f) Rate of hydrogen formation (brown).

Selectivity to the EOD pathway was first quantified by monitoring the H_2 oxidation current at a concentric Pt ring electrode (RRDE). Due to the presence of benzaldehyde (which will mainly decarbonylate on Pt to form surface-bound CO),[18–20] a special calibration was developed (Supplementary Discussion 1 and Figures S1-S9). Briefly, the collection efficiency (the fraction of the H_2 generated on the disk that can be detected by the ring), was determined by combining the hydrodynamic collection efficiency with a kinetic efficiency

for H_2 oxidation determined at 0.25 V, which was established to permit H_2 oxidation in the presence of benzaldehyde while yielding negligible steady state benzaldehyde oxidation. An overall collection efficiency of 7% was determined, and benzoate product was demonstrated to not affect this value.

The calibrated RRDE measurements are plotted in Figures 1b and 1c (see Figures S7-8 and Supplementary Discussion 2 for the raw disk and ring current data). The total disk currents during the forward and reverse sweeps from Figure 1a are (respectively) overlaid with the corresponding partial currents determined for the $1e^-$ EOD pathway (Equation S3). Gold favors H_2 production during benzaldehyde oxidation at low potentials. With increasing potential, the partial current to H_2 peaks at ~0.55 V and completely diminishes by 0.75 V. This is consistent on both the forward and reverse sweeps. In Figure 1d, the selectivity (S_{H2}) and Faradaic efficiency (FE) to the H_2 pathway are computed (Equations S1-9). We note that S_{H2} and FE in this system are not independent quantities since it is assumed that all current must go towards either EOD or ECO. Near the onset of activity, benzaldehyde oxidation appears almost completely selective to EOD, dropping off to negligible by about 0.7 V as was seen from the disk current. Using the H_2 selectivity, we calculate the molar product formation rates of carboxylate and hydrogen in Figures 1e and 1f. From this analysis, carboxylate formation (i.e., benzaldehyde oxidation) becomes mass transfer limited in aldehyde earlier (~0.68 V) than the upper plateau of the CV in Figure 1a (~0.8 V), replotted in Figure 1e for visual aid. This is a critical observation because it suggests that the selectivity to the EOD path does not fall (at least not primarily) due to local depletion of the reactant, but, rather, the change is first attributable to the growing favorability of discharging adsorbed H or breaking down formed H_2 at higher potentials. We thus return attention to the inflection in the CV at around 0.5 V (near the one-electron limiting current, Figure 1a). This is a similar potential region to the onset of OH_{ads} (0.5-0.6 V_{RHE}) on undercoordinated sites, which has been proposed to facilitate the onset of HOR on Au.[21,22]

While the RRDE measurement is in principle universal since it does not require the onset of mass transfer effects (fast kinetics) on the disk electrode, the calibration approach is not without its limitations (Supplementary Discussion 1). On the other hand, the Koutecký-Levich analysis is simpler and can validate the RRDE method, provided that a regime with at least partial mass transfer limitation can be reached. The Koutecký-Levich equation (equation 4) relates the measured current, *I*, to the limiting current (from Levich equation) and the kinetic current at a given potential, I_{kin}.

$$\frac{1}{\mathrm{I}} = \frac{1}{0.62\mathrm{nFA_{geom}D_{RCHO}^{2/3}\nu^{-1/6}\omega^{1/2}C_{RCHO}}} + \frac{1}{\mathrm{I_{kin}}} \qquad (4)$$

By fitting the measured current at each potential as a function of rotation rate, *n* is obtained from the slope of I^{-1} vs. $\omega^{-1/2}$ and in turn can be converted to a selectivity and Faradaic efficiency.

Figure 2a shows benzaldehyde oxidation at four different rotation rates. Mass transfer effects begin to appear by ~0.35 V (as indicated by separation of the curves), and full mass transfer limitation is reached by 0.75 V at all rotation rates. This is validated by Levich analysis of the limiting current regime (Figure S9). At potentials where mass transfer influence exists, we obtain *n* from the Koutecký-Levich equation (Equations S10-14). Above 0.4 V, the data fits the model very well and suggests that H_2 selectivity is independent of aldehyde mass transfer limitations, since there is no systematic RPM-dependent deviation from the line-of-best-fit (Figures S10-11). The average number of electrons transferred per benzaldehyde consumed is shown as a function of potential by the blue curve in Figure 2b (also in Figure S12 calculated with different values of D and v to assess the sensitivity to the assumed constants), where $n_{e^-} = 1$ represents the H_2 (EOD) pathway, and $n_{e^-} = 2$ represents the H_2O (ECO) pathway. Selectivity to the H_2 pathway decreases with rising potential, consistent with the RRDE analysis. Further, the Koutecký-Levich (blue curve) and RRDE (red curve) analyses largely agree quantitatively, suggesting both methods are viable for *in situ* quantification of H_2 selectivity.

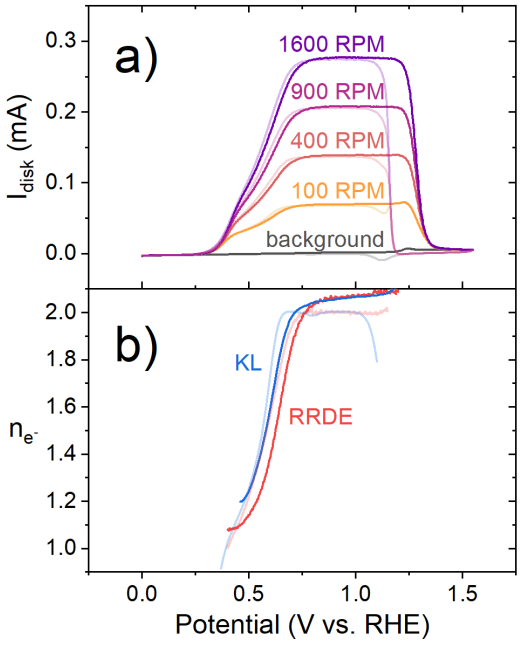

Figure 2. Au disk RDE study in 0.1 M NaOH + 1 mM benzaldehyde. Solid curves are from forward sweep; lighter curves are from reverse sweep. (a) CV overlay of different rotation rates (10 mV/s scan rate). (b) Average number of electrons transferred per aldehyde consumed according to Koutecký-Levich (KL, blue) and rotating ring disk electrode (RRDE, red) analysis.

Reaction on Ag

Analogous experiments were conducted with a Ag-disk Pt-ring RRDE in identical electrolyte (0.1 M NaOH, 1 mM benzaldehyde). Figure 3a shows the absence of a plateau in the 1600 RPM CV, indicating that the full mass transport limit is not reached. Instead, a mixed control regime is achieved, with partial control by mass transport indicated by rotation-dependence of the CV (Figure 4a). Benzaldehyde oxidation begins at ~0.2 V, has a shoulder at 0.5 V, and reaches a current peak at 0.7 V. At higher potentials, current decreases but does not drop off as sharply as with Au, suggesting that Ag retains some benzaldehyde oxidation activity despite accumulation of OH_{ads} and the onset of oxide formation.

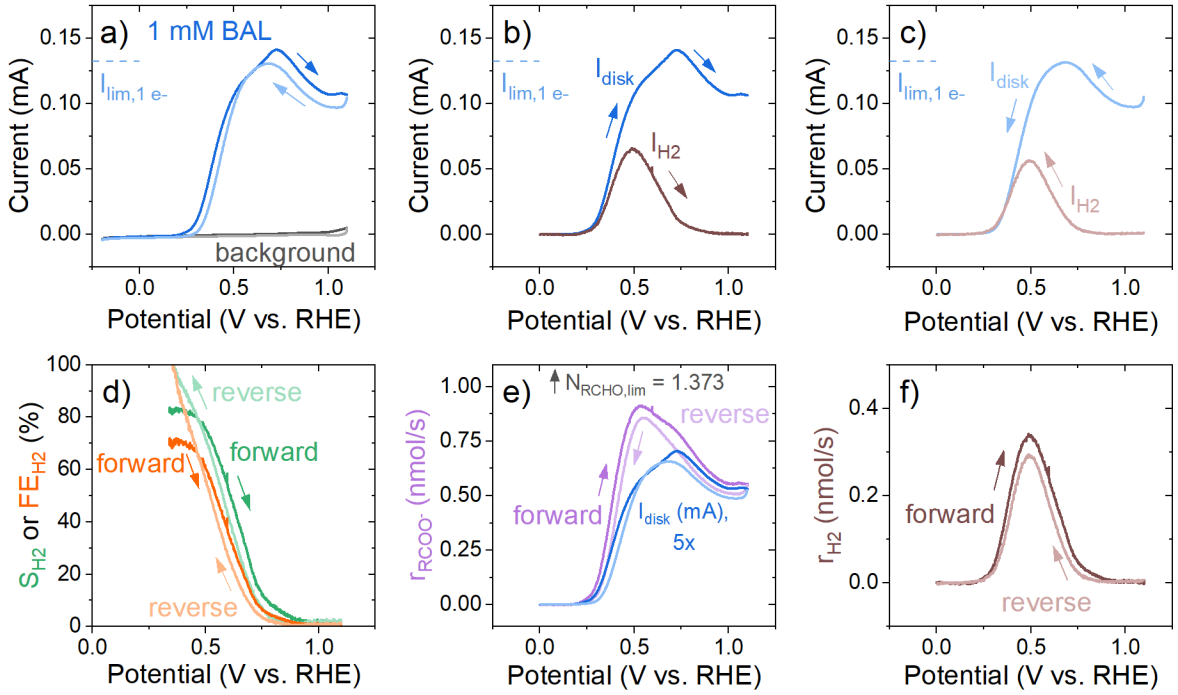

Figure 3. Ag disk - Pt ring RRDE measurements in 0.1 M NaOH + 1 mM benzaldehyde. Darker curves are forward sweep; lighter curves are reverse sweep. (a) Ag disk CV at 10 mV/s comparing background (black) and benzaldehyde (blue) in electrolyte at 1600 RPM. Dashed lines show the theoretical mass transfer limiting currents for the one-electron (H_2) and two-electron (H_2O) reaction pathways. (b) Forward sweep and (c) reverse sweep showing Ag disk current (blue) and partial current density to H_2 pathway (brown) calculated from Pt ring current. (d) Selectivity (green) and Faradaic efficiency (orange) to the one-electron (H_2) reaction pathway. (e) Rate of carboxylate product formation (purple); black dashed line is the maximum mass transfer rate of aldehyde to the surface; disk current (blue) is replotted for reference and rescaled for ease of comparison. (f) Rate of hydrogen formation (brown).

Figures 3b and 3c show the calibrated partial current to the H_2 pathway as well as the disk currents for the forward and reverse sweeps, respectively, from the CV in Figure 3a (see Figures S13-14 for the raw disk and ring current data). On both sweeps, the partial current to the H_2 pathway peaks at ~0.5 V and disappears around 0.8 V. Figure 3d shows the shift in selectivity (or Faradaic efficiency) from EOD to ECO with increasing potential, as was seen on Au. Below 0.5 V, the benzaldehyde oxidation is highly selective to H_2, while by 0.8 V, the H_2O-pathway is fully dominant. Figure 3e and 3f show the benzoate and hydrogen formation rates, respectively. Product formation rates are below the aldehyde mass transfer limit, with benzaldehyde oxidation activity maximizing near 0.53 V (contrast with the peak in disk current at 0.72 V). Therefore, like Au, the inflection in the Ag disk current at ~0.6 V can be explained by the change in electron efficiency of benzaldehyde conversion rather than increase in the benzoate formation rate (Figure 3e). The simultaneous decrease in benzoate formation rate and decrease in H_2 selectivity occur in a similar potential range as competitive OH_{ads} formation and/or oxidation of lower coordinated Ag sites.[23]

The RRDE results on Ag were validated with variation of rotation rate (Figure 4a) and Koutecký-Levich analysis (Figure 4b, Figures S15-18). Selectivity is in close agreement between the Koutecký-Levich (blue) vs. RRDE (red) methods between 0.4 and 1 V. In all cases, there is an uptick in current above 1 V that may be the onset of Ag oxidation and/or higher benzaldehyde oxidation activity.

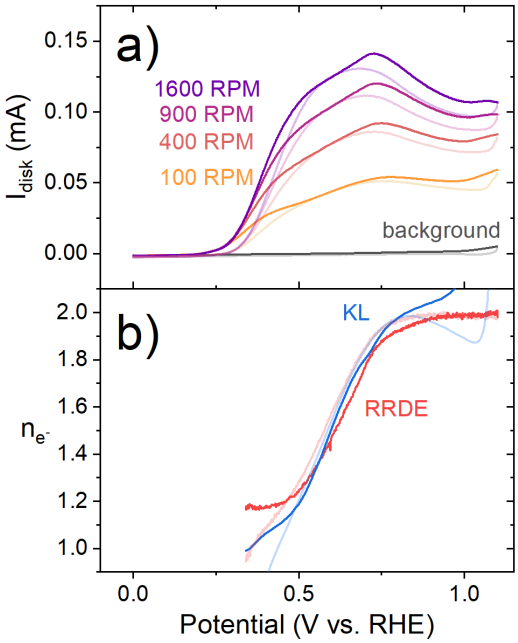

Figure 4. Ag disk RDE study in 0.1 M NaOH + 1 mM benzaldehyde. Solid curves are from forward sweep; lighter curves are from reverse sweep. (a) CV overlay of different rotation rates (10 mV/s scan rate). (b) Average number of electrons transferred per aldehyde consumed according to Koutecký-Levich (KL, blue) and rotating ring disk electrode (RRDE, red) analysis.

Reaction on Cu

Benzaldehyde oxidation activity and selectivity on Cu was also probed with RRDE. Cu has much lower activity compared to Au and Ag, so we performed experiments with 10 mM benzaldehyde to improve the signal-to-noise ratio of the Cu disk and Pt ring current. Figure 5 shows benzaldehyde oxidation at 1600 RPM on Cu compared to the background CV. The observed peak current (~53 μA) is far below that of the one-electron transfer mass transfer limiting current for 10 mM benzaldehyde (1325 μA), and the CVs are rotation rate-independent (not shown), indicating no mass transfer influence under the tested conditions. Therefore, the current is purely kinetic and Koutecký-Levich analysis could not be applied to Cu.

The benzaldehyde oxidation features on Cu are quite different than Au and Ag. Cu has a low onset potential (~0.05 V), slow increase in current up to 0.12 V, then a steady increase in current up to a peak at 0.4 V where current sharply drops and Cu oxidation begins. This is consistent with observations of other aldehyde oxidation reactions on Cu.[5,8,10] Notably, the background CV shows Cu oxidation to Cu(I) beginning at ~0.5 V, but the decrease in benzaldehyde oxidation current occurs at least 0.1 V before. This could suggest competitive adsorption of OH and/or the importance of lower coordinated sites which show oxidation prior to 0.5 V.[24] Notably, at higher potentials (not shown), higher Cu oxides are active for ECO, but anodic hydrogen has not been reported.[25,26]

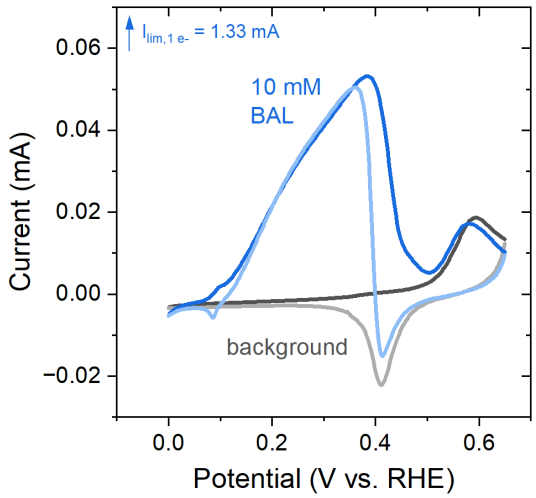

Figure 5. Cu disk CVs at 1600 RPM in 0.1 M NaOH comparing background (black) with 10 mM benzaldehyde (blue). The darker and lighter colored lines represent the forward and reverse sweep of the CV, respectively.

The ring current was also monitored during CV studies of Cu, but we had difficulty using RRDE collection to quantify anodic H_2. The CV without benzaldehyde shows a reductive current feature on the Pt ring at Cu disk potentials above 0.35 V (Figure S19). This

is attributed to oxidative Cu dissolution with reductive deposition onto the ring. This poses two issues: first, significant Cu deposition onto the Pt ring modifies the HOR kinetics, and second, the cathodic current shifts the Pt ring background current and interferes with H_2 detection above 0.35 V. Additionally, when not cycling Cu into the oxide formation region, we found Cu to have significantly lower activity that was difficult to quantify—i.e., frequent oxidation and reduction cycles seem to be necessary to keep the Cu surface clean and active. With these complicating factors, we were unable to accurately quantify the activity and selectivity towards anodic H_2 during benzaldehyde oxidation on Cu.

Nevertheless, we are still able to draw qualitative conclusions about EOD on Cu from the ring currents and to make comparisons to Ag and Au. Figure S20 compares the disk and ring current on the forward and reverse sweeps using Cu. At low potentials, we observe an increase in current on the Pt ring that coincides with an increase in Cu disk current for benzaldehyde oxidation, suggesting the formation of anodic H_2. The Pt ring current has a similar current shape profile as the Cu disk current, and the peak in ring current occurs at a similar potential as the peak disk current. Like Au and Ag, there is hysteresis in aldehyde oxidation activity between the forward and reverse sweeps due to the irreversibility of Cu oxide formation and reduction. Additionally, after Cu oxide reduction, the benzoate formation rate appears to briefly exceed that from the forward sweep. This aspect of the hysteresis is consistent with previous studies of formaldehyde oxidation on Cu using differential electrochemical mass spectrometry (DEMS).[4,8,27] The high initial rate upon reduction of the surface may be due to surface cleaning, roughening of the Cu, and/or aldehyde-mediated reduction.[28]

Discussion

The present data provides a direct comparison of EOD activity and selectivity on Au, Ag, and Cu under identical experimental conditions. Figure 6 compiles our benzaldehyde oxidation measurements across all three metals. Figure 6a shows RDE currents. Cu has an earlier onset potential by ~0.2 V compared to Au and Ag, and the reaction starts slightly earlier on Ag compared to Au.[5,9] Underscoring the trend, the Cu data was collected with 10 mM benzaldehyde yet still yield a lower peak current than Au and Ag at 1 mM. Figure 6b shows the benzoate product formation rates as a function of metal and potential (assuming there are no significant pathways other than benzaldehyde to benzoate). Since we were unable to accurately quantify anodic H_2 formed from Cu using RDE in this study, we estimated a best-case scenario of 100% Faradaic efficiency to H_2 (which previous works have reported, although these have been at higher pH[5,10]) for the sake of comparison. The peak benzoate formation rate follows in the order of Au > Ag >> Cu, which also generally agrees with trends reported in previous work, albeit across somewhat variable conditions and methods of surface area determination.[5,9] Benzoate formation rates on Au above 0.6 V reflect the mass transfer rate of aldehyde to the surface up to 1.3 V, where the inactive Au oxide appears. Ag becomes less active for benzaldehyde oxidation above 0.5 V, but its

surface oxide still exhibits some activity. In contrast, the first Cu oxide formed is also inactive. For all metals, the hydrogen formation rate peaks then falls with increasing potential due to catalyst deactivation and/or change in selectivity from the H_2 to H_2O pathway (Figure 6c). Selectivity to H_2 decreases with increasing potential in a similar manner on Au and Ag (Figure 6d), consistent with more favorable kinetics for Volmer-like oxidation at higher potentials (electrochemical process) versus Tafel-like combination (thermal process) of hydrogen atoms. Generally, Au and Ag will produce more H_2 per unit area than Cu above 0.25 V for a given benzaldehyde concentration due to a much higher benzoate formation rate while maintaining relatively high H_2 selectivity. Nevertheless, Cu-based catalysts may still show promise due to low cost and facile fabrication of high surface area substrates, as has been demonstrated by others.[5,10,11]

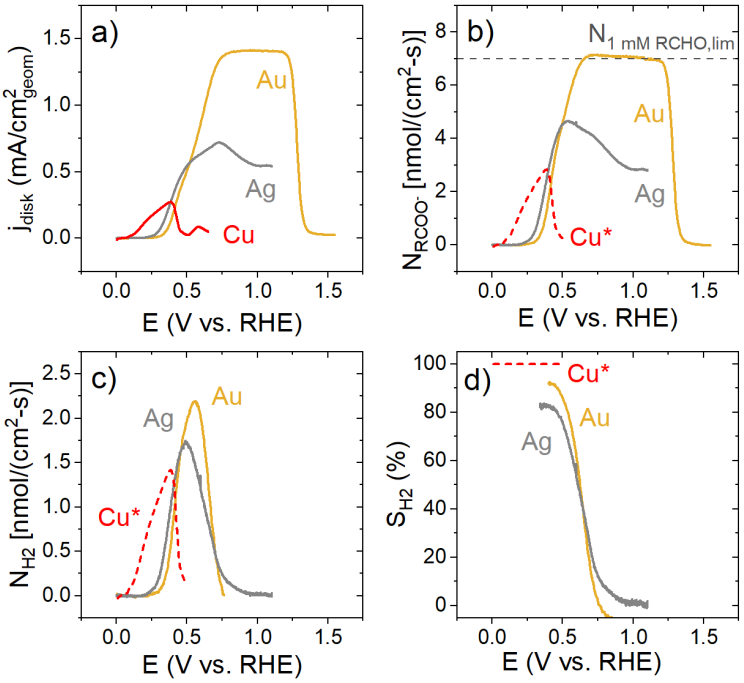

Figure 6. Au- (gold), Ag- (gray), or Cu- (red) disk Pt-ring RRDE in 0.1 M NaOH with 1 mM benzaldehyde (for Au and Ag) or 10 mM benzaldehyde (for Cu). For a conservative comparison, it was assumed that benzaldehyde oxidation had 100% Faradaic efficiency to the EOD pathway on Cu, indicated by the asterisk (*) and red dashed lines in b-d. Rates are normalized to the geometric area of the RDE, 0.196 cm^2). (a) Disk current during positive CV scan at 10 mV/s at 1600 RPM. (b) Benzoate formation rate during the forward sweep based on calibration of the disk and ring currents. Gray dashed line shows the mass transfer rate of 1 mM benzaldehyde to the disk surface at 1600 RPM. (c) H_2 formation rate during the forward sweep based on calibration of the Pt ring current. (d) Selectivity to the anodic H_2 pathway (i.e., one-electron, EOD).

Conclusion

In this contribution, we have characterized the benzaldehyde oxidation activity and H_2 selectivity of Au, Ag, and Cu under a common set of conditions. We find Cu to have a lower onset potential than Au and Ag by ~0.2 V. On the other hand, Au and Ag have much higher peak anodic H_2 and carboxylate formation rates at a given aldehyde concentration. The first oxides formed on Au and Cu are inactive while the first oxide on Ag is active for aldehyde oxidation. The selectivity to the one-electron EOD (H_2) pathway decreases with increasing potential. These results suggest that Au and Ag are worth further investigation despite higher overpotential requirements than Cu; overall, the operating potential is still quite low (<0.4 V) when comparing to OER, for example. Further kinetic studies and mechanistic investigations are required to identify the relevant catalyst and electrolyte design principles to optimize hydrogen and carboxylate production rates.

Additionally, we developed and validated two methods for *in situ* quantification of anodic H_2 selectivity during aldehyde electrooxidation. Despite the presence of aldehyde and carboxylates, a Pt collection electrode can oxidize hydrogen generated via EOD in an RRDE setup. With proper collection efficiency determination, Pt ring current can be converted into a partial disk current towards the EOD pathway. The RRDE method was validated by measuring benzaldehyde oxidation at different rotation rates and fitting the average number of electrons transferred per aldehyde consumed to the Koutecký-Levich equation. While Koutecký-Levich requires mass transfer limitations to be operant and requires multiple measurements at different RPMs, the theoretical basis provides high confidence in the results. Although quantitative RRDE analysis of EOD can be cumbersome, it has excellent time resolution and provides a straightforward indication of anodic H_2 generation. Thus, RDE may be used as a rapid assessment tool to simultaneously quantify H_2 selectivity and reaction kinetics of EOD *in situ*.

Acknowledgements

The authors acknowledge support from the Department of Energy (DE-SC0023424).

References

(1) Megía, P. J.; Vizcaíno, A. J.; Calles, J. A.; Carrero, A. Hydrogen Production Technologies: From Fossil Fuels toward Renewable Sources. A Mini Review. *Energy Fuels* **2021**, *35* (20), 16403–16415. https://doi.org/10.1021/acs.energyfuels.1c02501.

(2) You, B.; Liu, X.; Jiang, N.; Sun, Y. A General Strategy for Decoupled Hydrogen Production from Water Splitting by Integrating Oxidative Biomass Valorization. *J. Am. Chem. Soc.* **2016**, *138* (41), 13639–13646. https://doi.org/10.1021/jacs.6b07127.

(3) Ramos, N. C.; Holewinski, A. Recent Advances in Anodic Hydrogen Production: Electrochemical Oxidative Dehydrogenation of Aldehydes to Carboxylates. *Curr. Opin. Electrochem.* **2024**, 101484. https://doi.org/10.1016/j.coelec.2024.101484.

(4) Anastasijevic, N. A.; Baltruschat, H.; Heitbaum, J. On the Hydrogen Evolution during the Electrochemical Oxidation of Aldehydes at Ib Metals. *Electrochimica Acta* **1993**, *38* (8), 1067–1072. https://doi.org/10.1016/0013-4686(93)80214-K.

(5) Liu, H.; Agrawal, N.; Ganguly, A.; Chen, Y.; Lee, J.; Yu, J.; Huang, W.; Wright, M. M.; Janik, M. J.; Li, W. Ultra-Low Voltage Bipolar Hydrogen Production from Biomass-Derived Aldehydes and Water in Membrane-Less Electrolyzers. *Energy Environ. Sci.* **2022**, *15* (10), 4175–4189. https://doi.org/10.1039/D2EE01427K.

(6) Hasse, J. C.; Manyé Ibáñez, M.; Holewinski, A. Impact of Electrolyte Composition on Bulk Electrolysis of Furfural over Platinum Electrodes**. *ChemCatChem* **2023**, *15* (23), e202300988. https://doi.org/10.1002/cctc.202300988.

(7) Bełtowska-Brzezinska, M. Electrochemical Oxidation of Formaldehyde on Gold and Silver. *Electrochimica Acta* **1985**, *30* (9), 1193–1198. https://doi.org/10.1016/0013-4686(95)80012-3.

(8) Jusys, Z.; Vaškelis, A. Mass Spectrometric Cyclic Voltammetry of Copper in Alkaline Formaldehyde Solutions. *J. Electroanal. Chem.* **1992**, *335* (1), 93–104. https://doi.org/10.1016/0022-0728(92)80235-V.

(9) Van Den Meerakker, J. E. A. M. On the Mechanism of Electroless Plating. I. Oxidation of Formaldehyde at Different Electrode Surfaces. *J. Appl. Electrochem.* **1981**, *11* (3), 387–393. https://doi.org/10.1007/BF00613959.

(10) Wang, T.; Tao, L.; Zhu, X.; Chen, C.; Chen, W.; Du, S.; Zhou, Y.; Zhou, B.; Wang, D.; Xie, C.; Long, P.; Li, W.; Wang, Y.; Chen, R.; Zou, Y.; Fu, X. Z.; Li, Y.; Duan, X.; Wang, S. Combined Anodic and Cathodic Hydrogen Production from Aldehyde Oxidation and Hydrogen Evolution Reaction. *Nat. Catal.* **2021**, *5* (1), 66–73. https://doi.org/10.1038/s41929-021-00721-y.

(11) Liu, H.; Yu, J.; Chen, Y.; Lee, J.; Huang, W.; Li, W. Cu-Based Bimetallic Catalysts for Electrocatalytic Oxidative Dehydrogenation of Furfural with Practical Rates. *ACS Appl. Mater. Interfaces* **2023**, *15* (31), 37477–37485. https://doi.org/10.1021/acsami.3c06783.

(12) Bell, R. P. The Reversible Hydration of Carbonyl Compounds. In *Advances in Physical Organic Chemistry*; Gold, V., Ed.; Academic Press, 1966; Vol. 4, pp 1–29. https://doi.org/10.1016/S0065-3160(08)60351-2.

(13) Tiwari, A.; Maagaard, T.; Chorkendorff, I.; Horch, S. Effect of Dissolved Glassware on the Structure-Sensitive Part of the Cu(111) Voltammogram in KOH. *ACS Energy Lett.* **2019**, *4* (7), 1645–1649. https://doi.org/10.1021/acsenergylett.9b01064.
(14) Tashiro, K.; Kobayashi, M.; Nakajima, K.; Taketsugu, T. Computational Survey of Humin Formation from 5-(Hydroxymethyl)Furfural under Basic Conditions. *RSC Adv.* **2023**, *13* (24), 16293–16299. https://doi.org/10.1039/D3RA02870D.
(15) Lukas Krebs, M.; Bodach, A.; Wang, C.; Schüth, F. Stabilization of Alkaline 5-HMF Electrolytes via Cannizzaro Reaction for the Electrochemical Oxidation to FDCA. *Green Chem.* **2023**, *25* (5), 1797–1802. https://doi.org/10.1039/D2GC04732B.
(16) Komiyama, H.; Smith, J. M. Diffusivities of Benzaldehyde in Methanol-Water Mixtures. *J. Chem. Eng. Data* **1974**, *19* (4), 384–386. https://doi.org/10.1021/je60063a017.
(17) Sipos, P. M.; Hefter, G.; May, P. M. Viscosities and Densities of Highly Concentrated Aqueous MOH Solutions (M+ = Na+, K+, Li+, Cs+, (CH3)4N+) at 25.0 °C. *J. Chem. Eng. Data* **2000**, *45* (4), 613–617. https://doi.org/10.1021/je000019h.
(18) Avramov-Ivic, M.; Adzic, R. R.; Bewick, A.; Razaq, M. An Investigation of the Oxidation of Formaldehyde on Noble Metal Electrodes in Alkaline Solutions by Electrochemically Modulated Infrared Spectroscopy (Emirs). *J. Electroanal. Chem. Interfacial Electrochem.* **1988**, *240* (1), 161–169. https://doi.org/10.1016/0022-0728(88)80320-6.
(19) Román, A. M.; Hasse, J. C.; Medlin, J. W.; Holewinski, A. Elucidating Acidic Electro-Oxidation Pathways of Furfural on Platinum. *ACS Catal.* **2019**, *9* (11), 10305–10316. https://doi.org/10.1021/acscatal.9b02656.
(20) Hasse, J. C.; Agrawal, N.; Janik, M. J.; Holewinski, A. ATR-SEIRAS Investigation of the Electro-Oxidation Mechanism of Biomass-Derived C5 Furanics on Platinum Electrodes. *J. Phys. Chem. C* **2022**, *126* (16), 7054–7065. https://doi.org/10.1021/acs.jpcc.2c01259.
(21) Strmcnik, D.; Uchimura, M.; Wang, C.; Subbaraman, R.; Danilovic, N.; van der Vliet, D.; Paulikas, A. P.; Stamenkovic, V. R.; Markovic, N. M. Improving the Hydrogen Oxidation Reaction Rate by Promotion of Hydroxyl Adsorption. *Nat. Chem.* **2013**, *5* (4), 300–306. https://doi.org/10.1038/nchem.1574.
(22) Angerstein-Kozlowska, H.; Conway, B. E.; Hamelin, A. Electrocatalytic Mediation of Oxidation of H2 at Gold by Chemisorbed States of Anions. *J. Electroanal. Chem. Interfacial Electrochem.* **1990**, *277* (1), 233–252. https://doi.org/10.1016/0022-0728(90)85105-E.
(23) Blizanac, B. B.; Ross, P. N.; Marković, N. M. Oxygen Reduction on Silver Low-Index Single-Crystal Surfaces in Alkaline Solution: Rotating Ring DiskAg(Hkl) Studies. *J. Phys. Chem. B* **2006**, *110* (10), 4735–4741. https://doi.org/10.1021/jp056050d.
(24) Ngamchuea, K. An Overview of the Voltammetric Behaviour of Cu Single-Crystal Electrodes. *Curr. Opin. Electrochem.* **2023**, *37*, 101193. https://doi.org/10.1016/j.coelec.2022.101193.
(25) Nam, D.-H.; Taitt, B. J.; Choi, K.-S. Copper-Based Catalytic Anodes To Produce 2,5-Furandicarboxylic Acid, a Biomass-Derived Alternative to Terephthalic Acid. *ACS Catal.* **2018**, *8* (2), 1197–1206. https://doi.org/10.1021/acscatal.7b03152.

(26) Woo, J.; Moon, B. C.; Lee, U.; Oh, H.-S.; Chae, K. H.; Jun, Y.; Min, B. K.; Lee, D. K. Collaborative Electrochemical Oxidation of the Alcohol and Aldehyde Groups of 5-Hydroxymethylfurfural by NiOOH and Cu(OH)2 for Superior 2,5-Furandicarboxylic Acid Production. *ACS Catal.* **2022**, *12* (7), 4078–4091. https://doi.org/10.1021/acscatal.1c05341.

(27) Jusys, Z. H/D Substitution Effect on Formaldehyde Oxidation Rate at a Copper Anode in Alkaline Medium Studied by Differential Electrochemical Mass Spectrometry. *J. Electroanal. Chem.* **1994**, *375* (1), 257–262. https://doi.org/10.1016/0022-0728(94)03390-0.

(28) Preti, D.; Squarcialupi, S.; Fachinetti, G. Aerobic, Copper-Mediated Oxidation of Alkaline Formaldehyde to Fuel-Cell Grade Hydrogen and Formate: Mechanism and Applications. *Angew. Chem. Int. Ed.* **2009**, *48* (26), 4763–4766. https://doi.org/10.1002/anie.200805860.